RG on a Fermi surface

Evelyn Tang
(Dated: May 7, 2010)

We review the renormalization group (RG) method for interacting fermions, building off typical ϕ^4 theory to account for the presence of a Fermi surface. A few geometries and the general procedure are briefly discussed. The method is illustrated with a model of two Fermi circles with different spin components and momenta, which can describe experiments with interacting fermions. General results obtained from this method, such as implications for Fermi-liquid theory and the BCS instability, are summarized.

A. Introduction

The RG has been useful in treating interactions – both conceptually and as a method for removing high energy degrees of freedom. This is because critical behavior is assumed to be arise from the low energy degrees of freedom of the system. As a concept it arose in the 1950s and a decade later was applied to a lattice model by Kadanoff, and consolidated into its modern form with Wilson. In condensed matter physics it has since been applied to a variety systems and has been of great success in describing critical phenomena.

In this paper we assume familiarity with ϕ^4 theory for bosons, and review the modifications necessary to apply RG to fermions. We discuss dealing with a Fermi surface for a few dimensions and simple geometries, and outline the general procedure. Next we illustrate the method by applying it to two colliding Fermi surfaces, i.e. two surfaces displaced by momentum $2K_D$ and with different spin. The results are compared with those from the more typical case of two stationary surfaces. Lastly, we discuss the broader relevance of the RG and the scope of this technique.

I. RG FOR FERMIONS

The RG relies on the idea of scale invariance, in that distances or energies can be successively rescaled without loss of underlying physics, rather it allows the examination of the critical behavior of the system at certain fixed points. The basic ideas and methods of ϕ^4 scalar field theory can be applied to fermions, however anti-commutation rules and the presence of a Fermi surface demand a different treatment [1]. To this end Grassmann variables are introduced, which describe fermionic coherent states. Using the path-integral approach, the partition function at inverse temperature β can be mapped to a system of d spatial dimensions and width β in the imaginary time direction. Variables are written in the Fourier bases of frequency and momentum which give us an additional integral over all frequency values (at zero temperature $\omega \to \infty$). The unperturbed partition function is then

$$Z = \int \prod_i \prod_{|k|<\Lambda} d\bar{\psi}_i(\omega,k) d\psi_i(\omega,k) e^{S_0} \tag{1}$$

$$S_0 = \sum_i \int_{-\Lambda}^{\Lambda} \frac{d^d k}{(2\pi)^d} \int_{-\infty}^{\infty} d\omega\, \bar{\psi}_i(\omega,k)(-G^{-1}(\omega))\psi_i(\omega,k)$$

where $G(\omega)$ is the Green's function, Λ is the cutoff momentum and i labels each fermion. All other terms in the action will be taken as perturbations to the Gaussian action S_0.

A. With a Fermi Surface

In one-dimension the Fermi surface is simply two points, so the RG is very similar to that in quantum field theory where we shrink our phase space down to a point under renormalization. In two-dimensions the circular Fermi surface allows for a set of transitions that obey momentum conservation rules. Constraining ourselves to excitations at the Fermi surface, allowed transitions must have definite angular relations. In three-dimensions the physics is similar, only that the allowed angles have an additional degree of freedom and thus the allowed parameter space forms a line instead of a point. The non-rotationally invariant case differs from the rotationally invariant one where the coupling functions depend only on relative differences in scattering angle, while in the former they are now functions of the angles themselves. For nested Fermi surfaces, an additional scattering by the nested momentum vector is possible.

With a Gaussian action, we can use Wick's theorem to give us all possible pairings then integrate over the high-energy modes from Λ/s to Λ. Expanding the coupling functions in momentum and frequency, many couplings are found to be marginal at the tree-level renormalization and so we calculate those to the order of one-loop. Additional loops are supressed by an order of Λ/K_F and hence we have a solution as $\Lambda/K_F \to 0$; analogous to a $1/N$ expansion. As an extension from the cases discussed in [1], we now apply the RG to two Fermi surfaces with different spin and momenta. to illustrate in detail the method briefly outlined above.

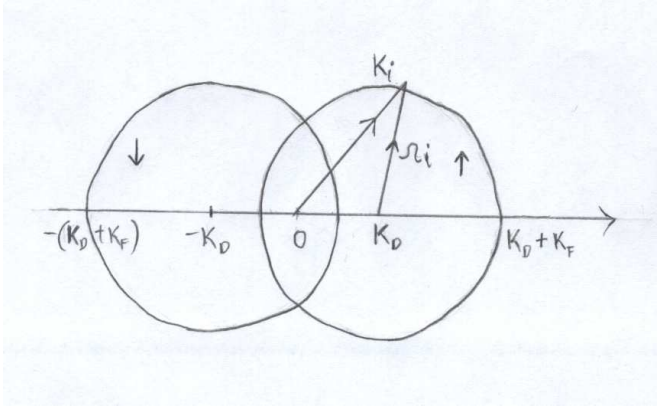

FIG. 1: Spin ↑ fermions move to the right with momentum $\mathbf{K_D}$ and spin ↓ ones move to the left with $-\mathbf{K_D}$. In [3] for example, this describes the collision of two atomic clouds.

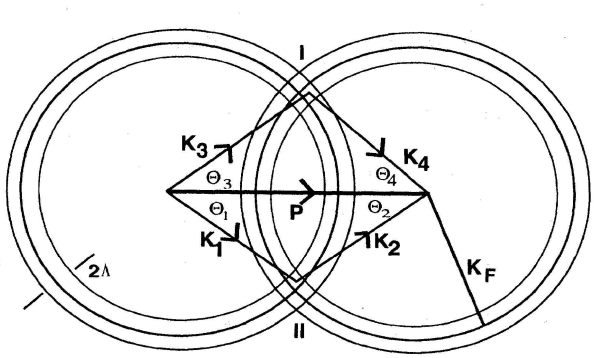

FIG. 2: A geometrical representation of scattering momenta that form solutions to Eq. 8. Case I and II are labelled in the diagram, while case III is when the two shells coalesce to sit atop each other. Figure taken from [1].

II. TWO COLLIDING FERMI GASES

Here we use the method briefly outlined above to study two interacting Fermi gases that have different spin and momenta. This gives us two Fermi surfaces each with radius K_F and separated by $2K_D$, see Fig. 1. There are several examples of this in two-dimensional electron gas or cold-atom systems.

In the former an applied magnetic field can change the momentum of a lower quantum well with respect to an upper well [2], corresponding to a displacement of its Fermi circle. For cold-atom systems, in recent work by Sommer et. al [3] two strongly interacting atomic clouds collide into each other, mix and form molecules . We use spin up ↑ and down ↓ as isospin labels for the degrees of freedom relevant to the sysem, e.g. in [3] the gases are Li-6 atoms in distinct hyperfine states. The calculation is done for the 2D case as in 3D only the angular phase space is increased while the physics does not change.

A. Tree-level calculation

As in Fig. 1, a fermion labelled i in this scheme carries momentum

$$\mathbf{K}_{i,\sigma} = \sigma\mathbf{K}_d + (K_F + k_i)\mathbf{\Omega_i} \tag{2}$$

where $\mathbf{\Omega}_i$ is a unit vector from the center of its Fermi circle to $\mathbf{K}_{i,\sigma}$. Near the ground state, we can linearize the dispersion relation near the Fermi surface as

$$\epsilon(K_i) = E(K_i) - \mu = vk_i \tag{3}$$

where v is the Fermi velocity. This gives $G^{-1} = vk - i\omega$. We write $d^dk = K_F k dk d\theta$ in Eq. 1 for each surface in the unperturbed action and proceed to consider the effects of interactions. For a quadratic perturbation written as

$$\delta S_2 = \sum_i \int_{-\Lambda}^{\Lambda} \frac{dk}{2\pi} \int_0^{2\pi} \frac{d\theta}{2\pi} \int_{-\infty}^{\infty} \frac{d\omega}{2\pi} \mu(k\omega)\bar{\psi}_i(\theta\omega k)\psi_i(\theta\omega k)$$

we can expand the coupling function μ

$$\mu(k,\omega) = \mu_{00} + \mu_{10}k + \mu_{01}i\omega + ... \tag{4}$$

The constant piece is a relevant perturbation that causes the Fermi sea to adjust to a change in the chemical potential, while the following two terms are marginal interactions that modify terms already present in the action. As none of this changes the physics and all other terms are irrelevant, we turn to the effect of a quartic perturbation:

$$\delta S_4 = \frac{1}{2!2!} \int_{K\omega\theta} \bar{\psi}(4)\bar{\psi}(3)\psi(2)\psi(1)u(4,3,2,1) \tag{5}$$

where $\bar{\psi}(i) = \bar{\psi}(K_i, \omega_i, \theta_i)$ etc.,

$$\int_{K\omega\theta} = \left[\prod_j^3 \int_0^{2\pi} \frac{d\theta_j}{2\pi} \int_{-\Lambda}^{\Lambda} \frac{dk_j}{2\pi} \int_{-\infty}^{\infty} \frac{d\omega_j}{2\pi}\right] \theta(\Lambda - |k_4|) \tag{6}$$

The step function in Eq. 6 results from evaluating the momentum conserving δ-function in the quartic interaction (Eq. 5), $\delta(\mathbf{K}_1 + \mathbf{K}_2 - \mathbf{K}_3 - \mathbf{K}_4)$ (momentum is conserved mod2π in a lattice problem).

As all four momenta are required to lie within an annulus of thickness 2Λ around the Fermi circle (see Fig. 2), the step function ensures that after choosing the first three momenta, the fourth is also constrained to lie within the cutoff Λ.

Expanding $u(4,3,2,1)$ similar to what we did for μ in Eq. 4, we find that the constant term u_0 is marginal and other terms are irrelevant. Further, the only allowed values of u_0 are

$$u_0 = u_{\uparrow\uparrow\uparrow\uparrow}\,,\, u_{\downarrow\downarrow\downarrow\downarrow}\,,\, u_{\uparrow\downarrow\uparrow\downarrow} = u_{\downarrow\uparrow\downarrow\uparrow} = -u_{\downarrow\uparrow\uparrow\downarrow} = -u_{\uparrow\downarrow\downarrow\uparrow} \tag{7}$$

as other couplings are forbidden by the Pauli principle and Wick's theorem. Here we take a coupling strength independent of spin.

For each coupling listed above, the $\mathbf{K}_D$'s cancel in the momentum δ-function which reduces to

$$\delta(\mathbf{\Omega}_1 + \mathbf{\Omega}_2 - \mathbf{\Omega}_3 - \mathbf{\Omega}_4) \tag{8}$$

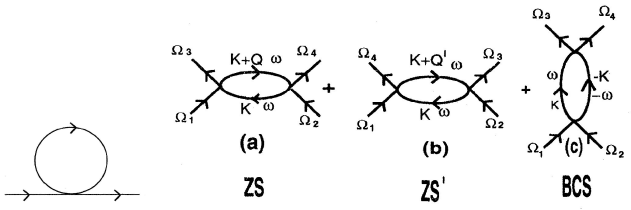

FIG. 3: Diagrams that contribute to one-loop corrections. The first is the tadpole graph that renormalizes the quadratic term, while the next three renormalize the quartic term. Figures taken from [1].

when we take $\Lambda/K_F \to 0$ after an infinite amount of renormalization. This is when all vectors lie on the Fermi surface at the fixed point.

There are only three solutions to Eq. 8:
Case I: $\mathbf{\Omega}_3 = \mathbf{\Omega}_1$ (hence $\mathbf{\Omega}_2 = \mathbf{\Omega}_4$) ,
Case II: $\mathbf{\Omega}_3 = \mathbf{\Omega}_2$ (hence $\mathbf{\Omega}_1 = \mathbf{\Omega}_4$) ,
Case III: $\mathbf{\Omega}_1 = -\mathbf{\Omega}_2$ (hence $\mathbf{\Omega}_3 = -\mathbf{\Omega}_4$) .
These constraints can be seen geometrically in Fig. 2 in the limit of zero shell thickness.

This gives us two independent functions, firstly in Case I and II (since u(Case I)$= -u$(Case II) as seen in Eq. 7), that we call $F(\theta_1 - \theta_2 \equiv \theta_{12})$ for forward scattering. The second is in Case III that we call $V(\theta_{13})$. These functions only depend on the difference between two angles due to rotational invariance. As they are both marginal at this level, we continue to the one-loop graphs.

B. One-loop corrections

The tadpole graph (Fig. 3) contributes to the quadratic term and acts as a shift in the chemical potential. However, we would like to maintain a fixed K_F as this corresponds to a fixed density of the system, so we solve for a term $\delta\mu$ in the chemical potential that reproduces itself under renormalization. This is obtained by solving the recursion relation self-consistently and consequently using that to modify G^{-1}.

The one-loop contribution to the quartic interaction u consists of three diagrams labelled ZS, ZS' and BCS respectively (Fig. 3) as obtained from the cumulant expansion. After evaluating the the δ functions for the conservation of momentum and frequency, and substituting the propagators, the corresponding integrals are

$$\begin{aligned} du(4321) = &\int_{-\infty}^{\infty}\int_{d\Lambda}\frac{d\omega dK}{4\pi^2}\int_0^{2\pi}\frac{d\theta}{2\pi}\frac{u(K+Q,3,K,1)u(4,K,2,K+Q)}{[i\omega - E(K)][i\omega - E(K+Q)]} \\ &-\int_{-\infty}^{\infty}\int_{d\Lambda}\frac{d\omega dK}{4\pi^2}\int_0^{2\pi}\frac{d\theta}{2\pi}\frac{u(K+Q',4,K,1)u(3,K,2,K+Q')}{[i\omega - E(K)][i\omega - E(K+Q')]} \\ &-\frac{1}{2}\int_{-\infty}^{\infty}\int_{d\Lambda}\frac{d\omega dK}{4\pi^2}\int_0^{2\pi}\frac{d\theta}{2\pi}\frac{u(P-K,K,2,1)u(4,3,P-K,K)}{[i\omega - E(K)][-i\omega - E(P+K)]} \end{aligned} \tag{9}$$

where $Q = K_3 - K_1$, $Q' = K_4 - K_1$ and $P = K_1 + K_2$. $\int_{d\Lambda}$ allows integration of loop momenta only in the shells being eliminated. This expression and the following discussion applies to each u in Eq. 7. Implications for the different spin couplings will be discussed at the end.

We begin with the renormalization of F (for $\mathbf{\Omega}_3 = \mathbf{\Omega}_1$). In the ZS diagram, $Q = 0$, however this diagram vanishes as both poles in the ω plane are on the same side. For the ZS' diagram, the allowed loop momenta fall within thin slices of order $d\Lambda^2/K_F$ (see Fig. 4). The ω integral also gives a denominator of order Λ, so that the total contribution to du is of order $(d\Lambda/\Lambda)(d\Lambda/K_F)$. Hence in the limit $dt = d|\Lambda|/\Lambda \to 0$, this contribution also vanishes. If we take instead $\mathbf{\Omega}_4 = \mathbf{\Omega}_1$, we obtain the same results with ZS↔ZS'.

In the BCS diagram the loop momenta suffer the same constraints as in the ZS' diagram, hence for the same kinematic reason this diagram does not contribute. Thus F is unchanged and remains a fixed point to this order.

In the renormalization of V, the ZS and ZS' diagrams have the same kinematic constraints cited above and are suppressed by $(d\Lambda/K_F)$. In the BCS diagram however, the loop angle runs over its full range. Regardless of the value of K in the shell, $P - K = -K$ will automatically also lie in the shell. The ω and k integrals produce a factor $dt = d|\Lambda|/\Lambda$ so we obtain the coupling function

$$\frac{dV(\theta_1 - \theta_3)}{dt} = -\frac{1}{8\pi^2}\int_0^{2\pi}\frac{d\theta}{2\pi}V(\theta_1 - \theta)V(\theta - \theta_3) \tag{10}$$

Using angular momentum eigenfunctions
$V_l = \int_0^{2\pi}\frac{d\theta}{2\pi}e^{il\theta}V(\theta)$, we can decompose Eq. 10 into flow equations for each angular momentum l:

$$\frac{dV_l}{dt} = -\frac{V_l^2}{4\pi} \tag{11}$$

This gives us the same flow equations as when $K_D = 0$, i.e. when the two Fermi surfaces coalesce and are stationary – however with different implications. For an attractive interaction, V_l is negative and we have a marginally

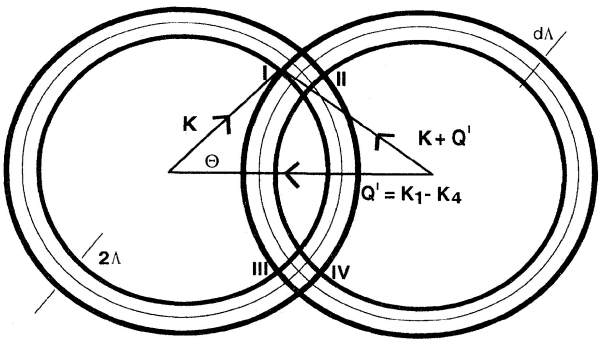

FIG. 4: Allowed values of loop momenta for the ZS' diagram in the renormalization of F. The requirement that the loop momenta come from the shell forces them to lie in an intersection region of width $(d\Lambda)^2$. Figure taken from [1].

relevant flow that opens a gap, corresponding to the BCS instability. This interaction creates Cooper pairs which we write in second quantized notation for clarity. For an interaction that mixes spin such as $u_{\uparrow\downarrow\uparrow\downarrow}$, the pair $\langle c^\dagger_{k+K_D,\uparrow} c^\dagger_{-k-K_D,\downarrow}\rangle$ has an antisymmetric spin wavefunction and zero center of mass momentum. It will form pairs with even values of angular momentum $l = 0, 2...$ so that the overall wavefunction remains antisymmetric.

For Cooper pairs formed from the same spin species, e.g. via the interaction $u_{\uparrow\uparrow\uparrow\uparrow}$, we get $\langle c^\dagger_{k+K_D,\uparrow} c^\dagger_{-k+K_D,\uparrow}\rangle$. Now the spin wavefunction can is symmetric and thus only the odd angular momentum values $l = 1, 3...$ are allowed. These pairs now have a center of mass momentum K_D (or $-K_D$ in the $\downarrow$ case) since the gas is moving at K_D.

For a repulsive interaction, the results are unchanged from when $K_D = 0$. V_l is positive and the flow becomes irrelevant, falling off logarithmically. However, the ZS and ZS' graphs for the renormalization of V, that were irrelevant, turn out to modify the relevant BCS coupling (the calculation is beyond the scope of this paper). They contribute a small negative BCS term so that a gap opens in any case, even when all values of V_l are repulsive. Nevertheless, the crossover to the BCS instability can be slow, and in the interim the fixed point described by F will control the physics. This picture and other details are presented in the discussion.

III. DISCUSSION

As mentioned previously, the interim physics controlled by the fixed point of F can characterize many systems and turns out to be a very useful picture. It is certainly valid where T_c for the superconductor is very small, the l value for pairs is very high, or when $V = 0$ altogether. It can provide a systematic approach to Fermi-liquid theory that was proposed by Landau and has been of great success in describing interacting fermions at very low temperatures, $T \ll K_F$. In this picture, we see that there are no phase transitions, however new parameters given by marginal couplings such as m^*, the renormalized mass, are obtained. We are able to relate physical properties like static compressibility or phenomena such as zero sound, to F and m^*. The RG provides new insight and additional tools for understanding the physics of interacting fermions at low energy scales.

Further, the RG allows us to compare the relevance of different interactions and the resulting fixed points or phase transitions. In superconductors, we see that the interelectron repulsion will be logarithmically reduced while the Cooper pair attraction grows. This explains why superconductivity can occur even when the bare Coloumb interaction is much stronger than the BCS interaction. The tools described in the paper can also calculate the formation of charge or spin density waves and other experimentally observed phenomena.

The RG has been effective and very useful not only in condensed matter physics but also in particle or astrophysics. It has provided important results and reveals key insights into the physics of strongly interacting systems. This is a useful technique that will certainly continue to be a vital tool for which to tackle problems.

I thank David Mross, Andrew Potter and Brian Swingle for helpful discussions.

[1] R. Shankar, Rev. Mod. Phys. **66**, 129 (1994).
[2] J. P. Eisenstein, T. J. Gramila, L. N. Pfeiffer, and K. W. West, Phys. Rev. B **44**, 6511 (1991).
[3] *Universal spin transport in a strongly interacting fermi gas*, URL `http://meetings.aps.org/link/BAPS.2010.MAR.Y31.8`.